

# Thermodynamic, Spectroscopic, and Computational Studies of Lanthanide Complexation with Diethylenetriaminepentaacetic Acid: Temperature Effect and Coordination Modes

Guoxin Tian,<sup>†</sup> Leigh R. Martin,<sup>‡</sup> Zhiyong Zhang,<sup>§</sup> and Linfeng Rao<sup>\*,†</sup>

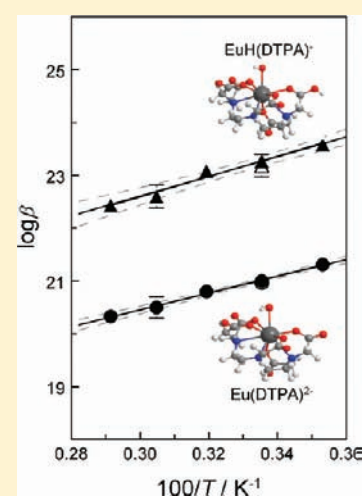
<sup>†</sup>Chemical Sciences Division, Lawrence Berkeley National Laboratory, Berkeley, California 94720, United States

<sup>‡</sup>Aqueous Separations and Radiochemistry Department, Idaho National Laboratory, PO Box 1625, Idaho Falls, Idaho 83415, United States

<sup>§</sup>Stanford Nanofabrication Facility, Stanford University, Stanford, California 94305, United States

**S** Supporting Information

**ABSTRACT:** Stability constants of two DTPA (diethylenetriaminepentaacetic acid) complexes with lanthanides ( $ML^{2-}$  and  $MHL^{-}$ , where M stands for Nd and Eu and L stands for diethylenetriaminepentaacetate) at 10, 25, 40, 55, and 70 °C were determined by potentiometry, absorption spectrophotometry, and luminescence spectroscopy. The enthalpies of complexation at 25 °C were determined by microcalorimetry. Thermodynamic data show that the complexation of  $Nd^{3+}$  and  $Eu^{3+}$  with DTPA is weakened at higher temperatures, a 10-fold decrease in the stability constants of  $ML^{2-}$  and  $MHL^{-}$  as the temperature is increased from 10 to 70 °C. The effect of temperature is consistent with the exothermic enthalpy of complexation directly measured by microcalorimetry. Results by luminescence spectroscopy and density functional theory (DFT) calculations suggest that DTPA is octa-dentate in both the  $EuL^{2-}$  and  $EuHL^{-}$  complexes and, for the first time, the coordination mode in the  $EuHL^{-}$  complex was clarified by integration of the experimental data and DFT calculations. In the  $EuHL^{-}$  complex, the Eu is coordinated by an octa-dentate H(DTPA) ligand and a water molecule, and the protonation occurs on the oxygen of a carboxylate group.



## 1. INTRODUCTION

With the strategy of partitioning and transmutation (P-T) in the advanced nuclear fuel cycle, the long-lived trivalent actinides (An(III)) are to be separated from the trivalent lanthanides (Ln(III)) and transmuted to short-lived or stable isotopes in nuclear reactors or accelerator-driven systems. The actinides must be separated from the lanthanides prior to the transmutation, because some isotopes of lanthanides produced as a result of  $^{235}\text{U}$  fission could interfere with the neutron balance in the transmutation process due to their high cross sections of neutron absorption.

It is an extremely challenging task to separate An(III) from Ln(III) because of their chemical similarities. A process, called TALSPEAK (trivalent actinide lanthanide separations by phosphorus-reagent extraction from aqueous complexes),<sup>1,2</sup> has been shown to be a promising option for achieving the An(III)/Ln(III) separation. Effective separations of An(III) from Ln(III) by TALSPEAK have been demonstrated in several pilot-scale operations. However, the fundamental chemistry underlying the separations remains unclear. For example, there are discrepancies between the experimentally measured distribution coefficients of

An(III) and Ln(III) under TALSPEAK conditions and those predicted by thermodynamic models using the stability constants of An(III)/Ln(III) complexes in the literature. For example, in the regions of  $pC_H$  (i.e.,  $-\log[H^+]$ ) above  $\sim 3.5$ , the measured distribution coefficients of An(III) and Ln(III) decrease while the model predicted values increase as  $pC_H$  becomes higher.<sup>3,4</sup>

To achieve accurate prediction and precise control of the behavior of actinides and lanthanides in the TALSPEAK process, it is necessary to determine the thermodynamic parameters of the reactions in the TALSPEAK system, including the complexation of lanthanides and actinides with lactic acid and diethylenetriaminepentaacetic acid (DTPA), two complexants in the aqueous phase that play essential roles in differentiating between the actinides and lanthanides. The effect of operating conditions (e.g., temperature) on the complexation must be evaluated. There have been a few studies on the complexation of lanthanides with DTPA but only at or near 25 °C.<sup>5–9</sup> Thermodynamic data for the complexation of An(III) and Ln(III) with DTPA are still very

Received: January 5, 2011

Published: March 04, 2011

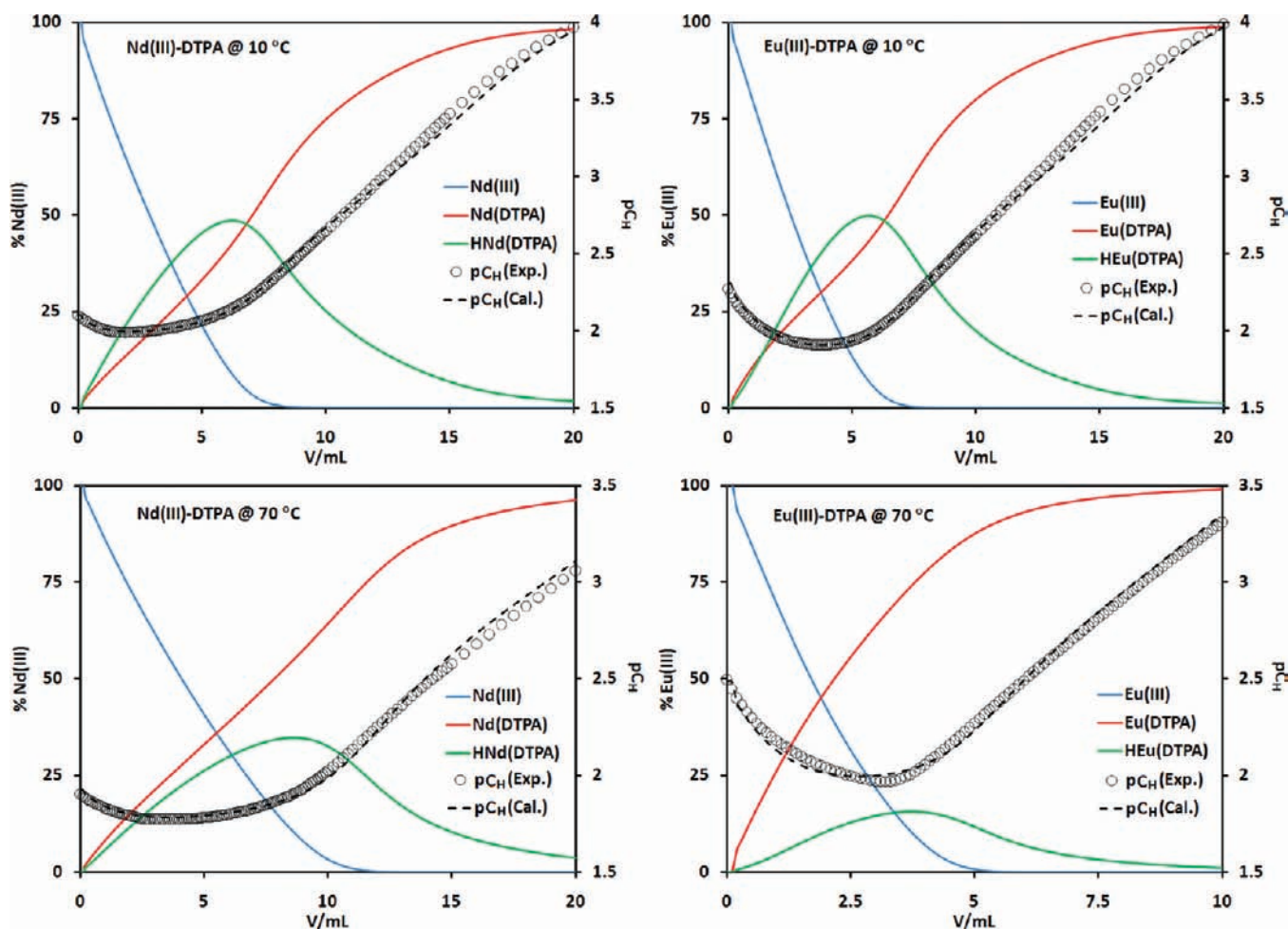


**Figure 1.** Potentiometric titrations of Nd(III)/DTPA and Eu(III)/DTPA complexation at 10 and 70 °C.  $I = 1.05 \text{ mol} \cdot \text{kg}^{-1} \text{ NaClO}_4$ ,  $V^0 = 20.0 \text{ mL}$ ,  $C_{\text{H}}^0/C_{\text{M}}^0/C_{\text{L}}^0$  (in  $\text{mmol} \cdot \text{dm}^{-3}$ ): 7.93/11.18/0 (upper left), 7.93/11.18/0 (lower left), 4.905/12.08/0 (upper right), 3.27/8.05/0 (lower right), titrant:  $0.05 \text{ mol} \cdot \text{dm}^{-3} \text{ Na}_3\text{H}_2\text{DTPA}$ . The left y-axis is for the percentages of Nd(III) or Eu(III) species; the right y-axis is for the pC<sub>H</sub> values.

scarce at temperatures above 25 °C. Consequently, it is very difficult to predict the behavior of actinides and lanthanides in the TALSPEAK process if the “envelope” of operating conditions (e.g., the temperature) changes. To help with the development of advanced An(III)/Ln(III) separation processes, we have started systematic studies on the thermodynamics of major reactions involved in TALSPEAK, including the protonation of lactate and DTPA,<sup>10</sup> the complexation of lanthanides and actinides with lactate,<sup>11</sup> and DTPA at different temperatures. Thermodynamic, spectroscopic, and computational techniques are used to reveal the effect of temperature on the complexation and the coordination modes in the lanthanide complexes. This paper summarizes the results on the complexation of lanthanides with DTPA.

## 2. EXPERIMENTAL SECTION

**2.1. Chemicals.** All chemicals were reagent grade or higher. Milli-Q water was used in preparations of all solutions. Stock solutions of Nd(III) perchlorate or Eu(III) perchlorate were prepared by dissolving Nd<sub>2</sub>O<sub>3</sub> or Eu<sub>2</sub>O<sub>3</sub> in perchloric acid (70%, Aldrich). The concentrations of lanthanides and perchloric acid in the stock solutions were determined by ethylenediaminetetraacetic acid (EDTA) complexometry<sup>12</sup> and Gran’s titration,<sup>13</sup> respectively. A stock solution of sodium diethylenetriaminepentaacetate was prepared by dissolving weighted amounts

of diethylenetriaminepentaacetic acid (Aldrich) in water and adding calculated quantities of NaOH to neutralize some of the protonated groups. The ionic strength of all working solutions was maintained at  $1.0 \text{ mol} \cdot \text{dm}^{-3}$  ( $\text{NaClO}_4$ ) at 25 °C. All the molar concentrations in this paper are referred to 25 °C.

**2.2. Potentiometry at Variable Temperatures.** Potentiometric experiments were carried out at 10, 25, 40, 55, and 70 °C for the complexation of Nd(III) and Eu(III) with DTPA using a variable-temperature titration setup. A detailed description of the apparatus and the procedures are provided elsewhere.<sup>14,15</sup> Electromotive force (EMF, in millivolts) was measured with a Metrohm pH meter (Model 713) equipped with a Ross combination pH electrode (Orion Model 8102). The original electrode filling solution (3.0 M KCl) was replaced with 1.0 M NaCl to avoid clogging of the electrode frit septum due to the low solubility of KClO<sub>4</sub>. The EMF of the glass electrode in the acidic and basic regions can be expressed by eqs 1 and 2.

$$E = E^0 + RT/F \ln[\text{H}^+] + \gamma_{\text{H}}[\text{H}^+] \quad (1)$$

$$E = E^0 + RT/F \ln(Q_w/[\text{OH}^-]) + \gamma_{\text{OH}}[\text{OH}^-] \quad (2)$$

where  $R$  is the gas constant,  $F$  is the Faraday constant, and  $T$  is the temperature in K.  $Q_w = [\text{H}^+][\text{OH}^-]$ . The last terms are the electrode junction potential ( $\Delta E_{\text{j,H}^+}$  or  $\Delta E_{\text{j,OH}^-}$ ) for the hydrogen ion (eq 1) or

**Table 1.** Thermodynamic Data on the Complexation of Nd(III) and Eu(III) with DTPA at Different Temperatures ( $I = 1.0 \text{ mol} \cdot \text{dm}^{-3} \text{ NaClO}_4$ )<sup>a</sup>

reaction	$t, ^\circ\text{C}$	method	$\log \beta_M$	$\log \beta_m$	$\Delta H, \text{kJ} \cdot \text{mol}^{-1}$	$\Delta S, \text{J} \cdot \text{K}^{-1} \cdot \text{mol}^{-1}$	ref
$\text{Nd}^{3+} + \text{L}^{5-} = \text{NdL}^{2-}$	10	pot	$20.48 \pm 0.05$	$20.62 \pm 0.06$			
		sp	$20.81 \pm 0.12$				
	25	pot,cal	$19.97 \pm 0.06$	$20.00 \pm 0.06$	$-28.0 \pm 0.06$	289	
		sp	$20.07 \pm 0.11$		$-26.9 \pm 0.06^b$		
			$21.62 \pm 0.02$		$-30.0$	312	5 <sup>c</sup>
	40	pot	$19.85 \pm 0.07$	$19.84 \pm 0.08$			
		sp	$19.87 \pm 0.15$				
	55	pot	$19.80 \pm 0.10$	$19.80 \pm 0.09$			
		sp	$19.85 \pm 0.15$				
	70	pot	$19.49 \pm 0.11$	$19.59 \pm 0.09$			
		sp	$19.73 \pm 0.14$				
	$\text{Nd}^{3+} + \text{H}^+ + \text{L}^{5-} = \text{NdHL}^+$	10	pot	$22.80 \pm 0.05$	$22.81 \pm 0.07$		
sp			$22.91 \pm 0.14$				
25		pot,cal	$22.20 \pm 0.04$	$22.14 \pm 0.07$	$-32.2 \pm 0.06$	317	
		sp	$22.16 \pm 0.13$		$-33.1 \pm 0.06^b$		
			24.01				5 <sup>c</sup>
40		pot	$21.99 \pm 0.05$	$21.86 \pm 0.07$			
		sp	$21.82 \pm 0.14$				
55		pot	$21.81 \pm 0.08$	$21.70 \pm 0.08$			
		sp	$21.66 \pm 0.15$				
70		pot	$21.68 \pm 0.08$	$21.57 \pm 0.08$			
		sp	$21.55 \pm 0.14$				
$\text{Eu}^{3+} + \text{L}^{5-} = \text{EuL}^{2-}$		10	pot	$21.31 \pm 0.10$	$21.29 \pm 0.10$		
	25	pot,cal	$21.00 \pm 0.08$	$20.96 \pm 0.10$	$-33.6 \pm 0.06$	290	
		lum	$20.97 \pm 0.19$		$-30.8 \pm 0.06^b$		
			$22.39 \pm 0.08$		$-32$	320	5 <sup>c</sup>
	40	pot	$20.80 \pm 0.16$	$20.78 \pm 0.16$			
	55	pot	$20.50 \pm 0.20$	$20.48 \pm 0.20$			
70	pot	$20.33 \pm 0.17$	$20.31 \pm 0.17$				
$\text{Eu}^{3+} + \text{H}^+ + \text{L}^{5-} = \text{EuHL}^+$	10	pot	$23.58 \pm 0.11$	$23.54 \pm 0.11$			
	25	pot,cal	$23.27 \pm 0.11$	$23.18 \pm 0.12$	$-37.3 \pm 0.06$	321	
		lum	$22.18 \pm 0.21$		$-36.7 \pm 0.06^b$		
			24.54				5 <sup>c</sup>
	40	pot	$23.08 \pm 0.19$	$23.04 \pm 0.19$			
	55	pot	$22.60 \pm 0.22$	$22.56 \pm 0.22$			
70	pot	$22.43 \pm 0.19$	$22.39 \pm 0.19$				

<sup>a</sup>The values of  $\log \beta_m$  for Nd(III)/DTPA complexes were calculated with eq 2 from the average of the two values obtained by potentiometry and spectrophotometry. <sup>b</sup>Values of  $\Delta H$  obtained by Van't Hoff equation. <sup>c</sup>For  $I = 0.1 \text{ mol} \cdot \text{dm}^{-3} \text{ KClO}_4$ . Methods: pot, potentiometry; sp, spectrophotometry; cal, calorimetry; lum, luminescence spectroscopy.

the hydroxide ion (eq 2), assumed to be proportional to the concentration of the hydrogen or hydroxide ions. In this work, the potentiometric titrations were conducted in the acidic region ( $-\log[\text{H}^+] < 5$ ). Therefore, the correction for the electrode junction potential of the hydroxide ion was negligible. Prior to each titration, an acid/base titration with standard perchloric acid and sodium hydroxide was performed to obtain the electrode parameters of  $E^0$  and  $\gamma_{\text{H}}$ . These parameters allowed the calculation of hydrogen ion concentrations from the EMF's in the subsequent titration.

In a typical titration, a solution (about 20 mL) containing appropriate amounts of lanthanides (Nd(III) or Eu(III)) was titrated with a solution of DTPA. The EMF data were collected at time intervals determined by the data collection criterion, i.e., the drift of EMF ( $\Delta E$ ) was less than 0.1 mV for 180 s. Fifty to seventy data points were collected in each titration. Multiple titrations were conducted at each temperature with

solutions of different concentrations of  $\text{C}_M^0$ ,  $\text{C}_L^0$ , and  $\text{C}_H^0$ . The stability constants of Nd(III)/DTPA and Eu(III)/DTPA complexes on the molarity scale were calculated with the program Hyperquad.<sup>16</sup> To allow comparison at different temperatures, the constants in molarity were converted to the constants in molality according to eq 3.<sup>17</sup>

$$\log_{10} K_m = \log_{10} K_M + \sum_r \nu_r \log_{10} \vartheta \quad (3)$$

where  $K_m$  and  $K_M$  are the equilibrium constants of a reaction in molality and molarity, respectively,  $\vartheta$  is the ratio of the values of molality to molarity for the specific ionic medium and equals  $1.05 \text{ dm}^3$  of solution per kg of water for 1.0 M  $\text{NaClO}_4$  at 25  $^\circ\text{C}$ , and  $\sum_r \nu_r$  is the sum of the stoichiometric coefficients of the reaction ( $\nu_r$  is positive for products and negative for reactants) and is equal to  $-1$  and  $-2$  for the complexation reactions of ( $\text{M}^{3+} + \text{L}^{5-} = \text{ML}^{2-}$ ) and ( $\text{M}^{3+} + \text{H}^+ + \text{L}^{5-} = \text{MHL}^+$ ), respectively.

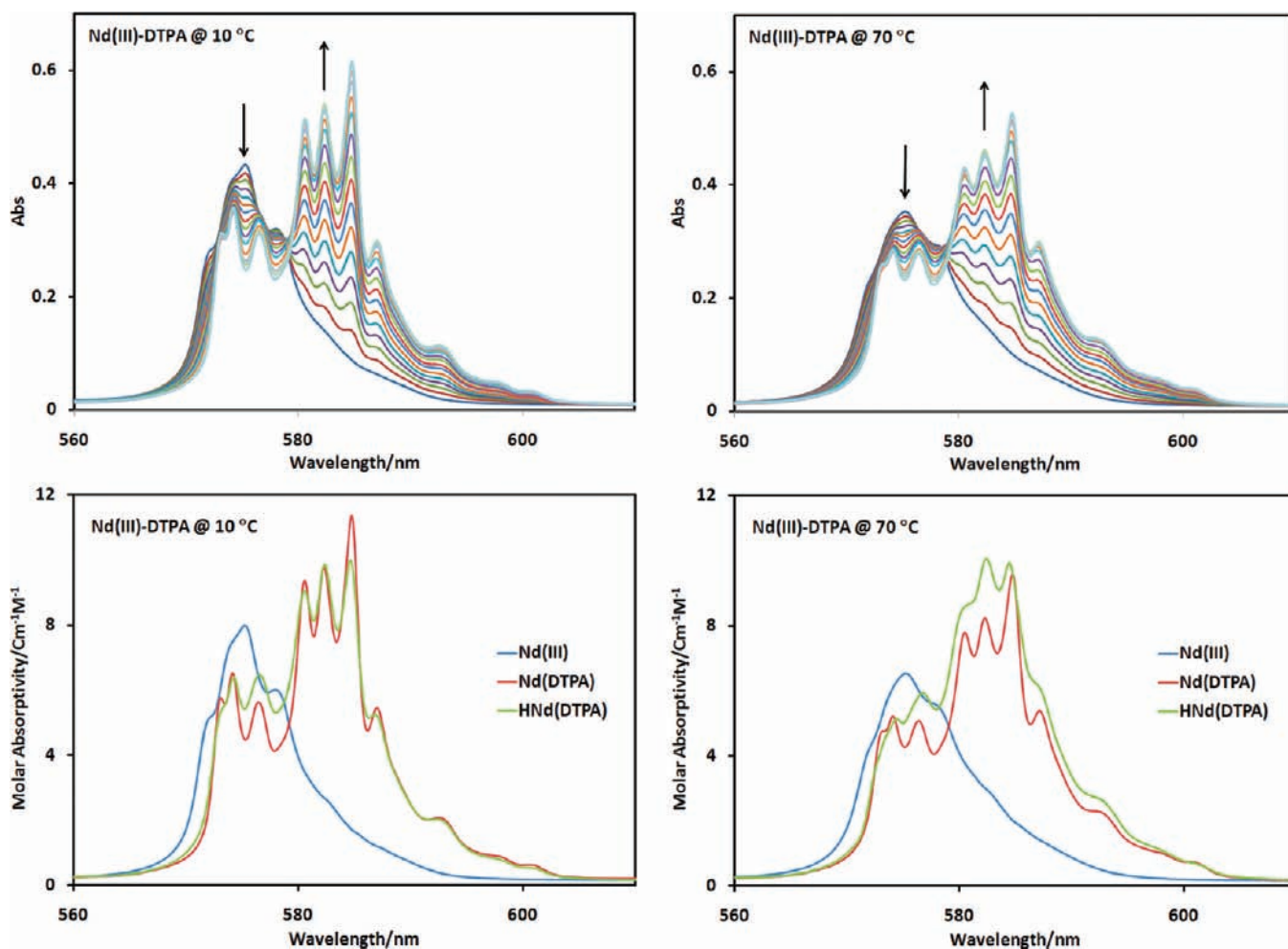


**Figure 2.** Representative spectrophotometric titrations of Nd(III)/DTPA complexation.  $I = 1.05 \text{ mol} \cdot \text{kg}^{-1} \text{ NaClO}_4$ . (Upper figures) Normalized absorption spectra of the titrations at 10 and 70 °C. Initial solution in cuvette: 2.75 mL,  $0.055 \text{ mol} \cdot \text{dm}^{-3} \text{ Nd}(\text{ClO}_4)_3 / 0.0055 \text{ mol} \cdot \text{dm}^{-3} \text{ HClO}_4$ ; titrant:  $0.233 \text{ mol} \cdot \text{dm}^{-3} \text{ Na}_4\text{HDTPA}$ . (Lower figures) Calculated molar absorptivity of  $\text{Nd}^{3+}$  and Nd(III)/DTPA complexes.

**2.3. Spectrophotometric Titrations at Variable Temperatures.** Absorption spectra of Nd(III) (550–600 nm, 0.1 nm interval) were collected on a Varian Cary-6000i spectrophotometer equipped with sample holders that were maintained at constant temperatures. Ten mm quartz cells were used. Multiple titrations with different concentrations of Nd(III) were performed. The initial concentrations of Nd(III) in the cells were around 0.05 M. In each titration, appropriate aliquots of the titrant (0.2 M DTPA) were added into the cell and mixed thoroughly (for 1 to 2 min) before the spectrum was collected. The mixing time was found to be sufficiently long for the complexation to be complete. Usually 15–20 additions were made, generating a set of 15–20 spectra in each titration. The stability constants of the Nd(III)/DTPA complexes (on the molarity scale) were calculated by nonlinear least-squares regression using the Hyperquad program.

**2.4. Microcalorimetry at 25 °C.** Calorimetric titrations were conducted with an isothermal microcalorimeter (Model ITC 4200, Calorimetry Sciences Corp.) at 25 °C. Procedures and results of the calibration of the calorimeter were provided elsewhere.<sup>14,18</sup>

Solutions of Nd(III) or Eu(III) (0.9 mL) were placed in the titration vessel and titrated with DTPA. Multiple titrations with different concentrations of Nd(III) or Eu(III) were performed to reduce the uncertainty. In a typical titration,  $n$  additions of the titrant were made (usually  $n = 40\text{--}50$ ), resulting in  $n$  experimental values of the total heat generated in the titration vessel ( $Q_{\text{ex},j}$ ,  $j = 1$  to  $n$ ). These values were

corrected for the heats of dilution of the titrant ( $Q_{\text{dil},j}$ ) that were determined in separate runs. The net reaction heat at the  $j$ -th point ( $Q_{r,j}$ ) was obtained from the difference:  $Q_{r,j} = Q_{\text{ex},j} - Q_{\text{dil},j}$ . The value of  $Q_{r,j}$  is a function of the concentrations of the reactants ( $C_M$ ,  $C_H$ , and  $C_{\text{DTPA}}$ ), the equilibrium constants, and the enthalpies of the reactions that occurred in the titration. A least-squares minimization program, Letagrop,<sup>19</sup> was used to calculate the enthalpy of complexation of Nd(III) or Eu(III) with DTPA.

**2.5. Luminescence Spectroscopy.** Luminescence emission spectra and lifetime of Eu(III) in aqueous solutions ( $[\text{Eu(III)}] = 2 \text{ mM}$ ,  $[\text{DTPA}] = 0\text{--}3.3 \text{ mM}$ ) were acquired on a HORIBA Jobin Yvon IBH FluoroLog-3 fluorometer adapted for time-resolved measurements. Ten mm quartz cells were used. A submicrosecond Xenon flash lamp (Jobin Yvon, 5000XeF) was the light source, and it was coupled to a double grating excitation monochromator for spectral selection. The input pulse energy (100 nF discharge capacitance) was about 50 mJ, and the optical pulse duration was less than 300 ns at fwhm. A thermoelectrically cooled single photon detection module (HORIBA Jobin Yvon IBH, TBX-04-D) that incorporates a fast rise time PMT, a wide bandwidth preamplifier, and a picosecond constant fraction discriminator was used as the detector. Signals were acquired using an IBH Data Station Hub, and data were analyzed using the commercially available DAS 6 decay analysis software package from HORIBA Jobin Yvon IBH. The goodness of fit was assessed by



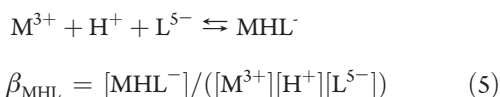
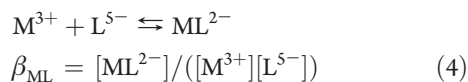
minimizing the reduced function,  $\chi^2$ , and visually inspecting the weighted residuals. Each trace contained at least 10 000 points, and the reported lifetime values resulted from at least three independent measurements.

**2.6. Density Functional Theory Calculations.** To help identify the coordination mode of DTPA in the protonated Eu(III) complex,  $\text{EuHL}^-$ , density functional theory (DFT) calculations were carried out to optimize the structures of  $\text{EuHL}^-$  complexes. The calculations were performed with the generalized gradient approximation exchange and correlation functional<sup>20</sup> using the NWChem program suite.<sup>21</sup> In the calculations, we used the Stuttgart\_RSC\_1997\_ECP effective core potential and basis set for Eu, the Stuttgart\_RLC\_ECP effective core potential<sup>22</sup> and basis set for C, N, and O, and the DZVP\_(DFT\_Orbital) basis set for H in the Basis Set Library<sup>23</sup> of the Environmental Management Sciences Laboratory (EMSL).

### 3. RESULTS

**3.1. Stability Constants of Nd(III)/DTPA and Eu(III)/DTPA at Different Temperatures.** The stability constants of Nd(III)/DTPA complexes at different temperatures were determined with potentiometry and spectrophotometry, while those of Eu(III)/DTPA complexes were determined with potentiometry and luminescence spectroscopy.

*Nd(III)/DTPA and Eu(III)/DTPA Complexes: Potentiometry.* Representative potentiometric titrations (at 10 and 70 °C, respectively) for Nd(III)/DTPA and Eu(III)/DTPA are shown in Figure 1. The best fit of the data by the Hyperquad program indicates that two monomeric Nd(III)/DTPA or Eu(III)/DTPA complexes, ML and MHL, form during the titration. The complexation reactions and equilibrium constants are represented by reactions 4 and 5,



where  $\text{M}^{3+}$  stands for  $\text{Nd}^{3+}$  or  $\text{Eu}^{3+}$  and  $\text{L}^{5-}$  stands for the fully deprotonated DTPA. The stability constants on the molarity scale at different temperatures were calculated by Hyperquad and are listed Table 1.

*Nd(III)/DTPA Complexes: Spectrophotometry.* Figure 2 shows the absorption spectra of two representative titrations for Nd(III)/DTPA complexation at 10 and 70 °C. The absorption band around 575 nm corresponds to the hypersensitive  $^4\text{I}_{9/2} \rightarrow ^4\text{G}_{5/2}$ ,  $^2\text{G}_{7/2}$  transition of Nd(III) that is sensitive to the coordination environment.<sup>24–27</sup> At each temperature, significant changes in the absorption spectra were observed as the concentration of DTPA was increased. In particular, the absorption in the region of 580–590 nm was greatly intensified and sharp branches of the band appeared (Figure 2). Analysis by the Hyperquad program indicated that there are three absorbing species of Nd(III) and the spectra were best-fitted with the formation of two Nd(III)/DTPA complexes,  $\text{NdL}^{2-}$  and  $\text{NdHL}^-$ , described by reactions 4 and 5, respectively. The molar absorptivities of free  $\text{Nd}^{3+}$ ,  $\text{NdL}^{2-}$ , and  $\text{NdHL}^-$  at 10 and 70 °C calculated by Hyperquad are depicted in the lower part of Figure 2. The spectra and absorptivities at other temperatures are not shown, but the trends in the spectra features are similar at each temperature. The

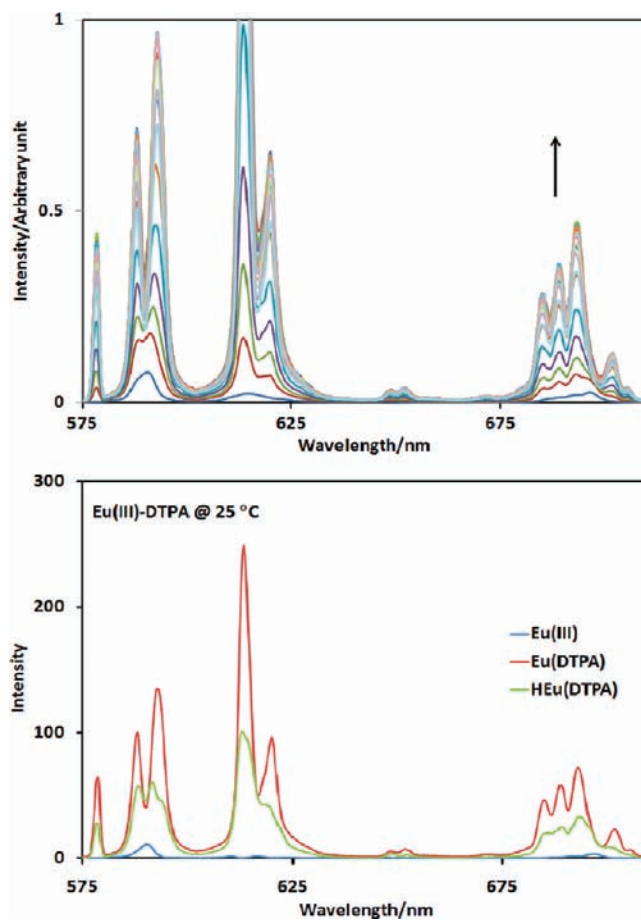


**Figure 3.** Normalized luminescence emission spectra (upper) and deconvoluted luminescence spectra for Eu(III) species (lower).  $t = 25$  °C,  $I = 1.00 \text{ mol} \cdot \text{dm}^{-3} \text{ NaClO}_4$ ,  $V^0 = 2.50 \text{ mL}$ ,  $C_{\text{H}}^0 = 1.3 \text{ mmol} \cdot \text{dm}^{-3}$ ,  $C_{\text{Eu}}^0 = 8.05 \text{ mmol} \cdot \text{dm}^{-3}$ ; titrant:  $50 \text{ mmol} \cdot \text{dm}^{-3} \text{ Na}_3\text{H}_2\text{DTPA}$ ; excitation wavelength: 394 nm.

stability constants of  $\text{NdL}^{2-}$  and  $\text{NdHL}^-$  determined by spectrophotometry are in excellent agreement with those determined by potentiometry, as shown in Table 1.

*Eu(III)/DTPA Complexes: Luminescence Spectroscopy.* The luminescence emission spectra of Eu(III)/DTPA solutions at 25 °C are shown in Figure 3. The spectra contains features originating from electronic transitions from the lowest excited state,  $^5\text{D}_0$ , to the ground state manifold,  $^7\text{F}_J$  ( $J = 0, 1, 2, 3, \dots$ ). As the concentration of DTPA was increased from 0 to 3.3 mM, the intensities of all luminescence bands increased significantly. The emission spectra were analyzed with Hyperquad, in the same way as in the processing of the absorption spectra for Nd(III)/DTPA, to obtain the stability constants of the Eu(III)/DTPA complexes. As compared in Table 1, the stability constants of  $\text{EuL}^{2-}$  and  $\text{EuHL}^-$  at 25 °C obtained by luminescence are in excellent agreement with those by potentiometry.

**3.2. Enthalpy of Complexation for Nd(III)/DTPA and Eu(III)/DTPA Complexes.** Figure 4 shows representative calorimetric titrations. Using the data from multiple titrations with different reagent concentrations in conjunction with the stability constants obtained by potentiometry and spectrophotometry, the enthalpies of complexation at 25 °C were calculated. The enthalpy values, as well as the entropies of complexation accordingly calculated, are summarized in Table 1.

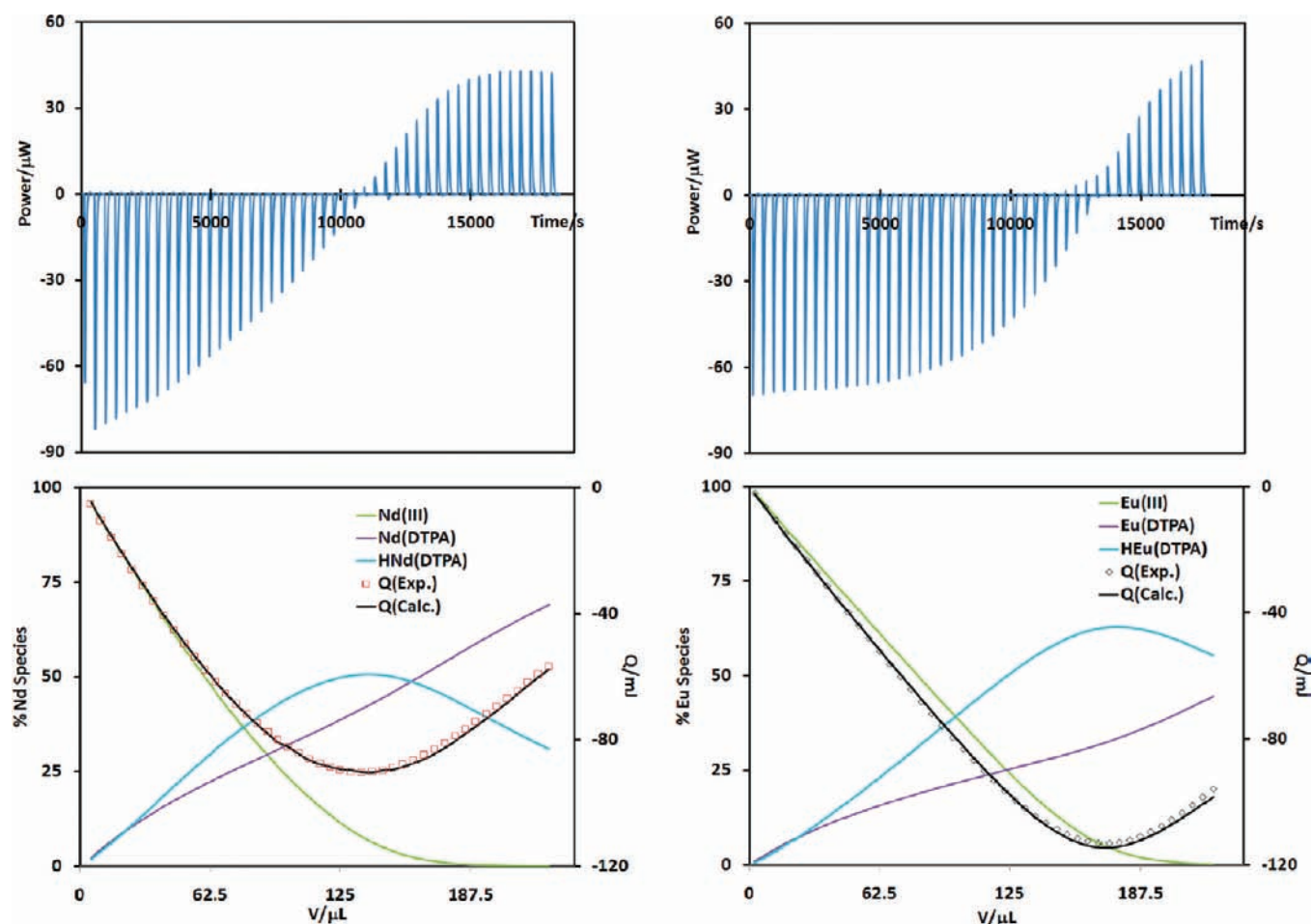


**Figure 4.** Calorimetric titrations of Nd(III)/DTPA (left) and Eu(III)/DTPA (right) complexation,  $t = 25\text{ }^{\circ}\text{C}$ ,  $I = 1.00\text{ mol}\cdot\text{dm}^{-3}\text{ NaClO}_4$ ,  $V^0 = 0.900\text{ mL}$ ; titrant:  $0.05\text{ M Na}_3\text{H}_2\text{DTPA}$  in  $1\text{ M NaClO}_4$ . Initial concentrations ( $C_{\text{H}}^0/C_{\text{M}}^0$  in  $\text{mmol}\cdot\text{dm}^{-3}$ ): 4.4/6.2 (left); 3.6/8.9 (right). The upper figures are the thermograms of the titrations.

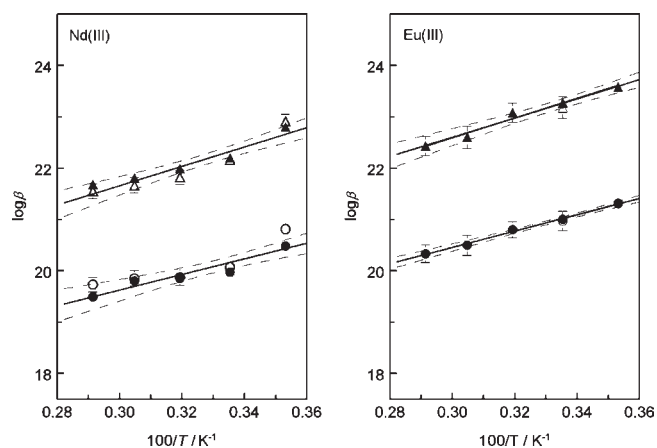


**Figure 5.** Van't Hoff plot of the stability constants of Nd(III)/DTPA (left) and Eu(III)/DTPA (right) complexes.  $I = 1.05\text{ mol}\cdot\text{kg}^{-1}\text{ NaClO}_4$ . (●) ML, (▲) MHL where M stands for Nd or Eu and L stands for DTPA. Solid symbols, data from potentiometry; open symbols, data from absorption spectroscopy (for Nd) or luminescence spectroscopy (for Eu). Solid lines represent the linear fits weighted by uncertainty; dashed lines represent the upper and lower limits of a confidence band at the 95% level.

In comparison, the stability constants of Nd(III)/DTPA and Eu(III)/DTPA at different temperatures are plotted as functions

of  $1/T$  (Figure 5). The linear correlations between  $\log \beta$  and  $1/T$  suggest that the effect of temperature on the complexation could be approximately described with the constant enthalpy approach in the temperature range of  $10\text{--}70\text{ }^{\circ}\text{C}$ . From the slopes of the linear fits, the enthalpies of complexation (in  $\text{kJ}\cdot\text{mol}^{-1}$ ) for reactions 4 and 5 were calculated to be  $-26.9$  ( $\text{NdL}^{2-}$ ),  $-30.8$  ( $\text{EuL}^{2-}$ ),  $-33.1$  ( $\text{NdHL}^-$ ), and  $-36.7$  ( $\text{EuHL}^-$ ), respectively. These values compare well with those directly determined by microcalorimetry (Table 1).

### 3.3. Luminescence Lifetime of Eu(III)/DTPA Solutions.

Figure 6 shows the luminescence decay of Eu(III)/DTPA solutions at  $25\text{ }^{\circ}\text{C}$ . It is evident that, as the concentration of DTPA is increased (from Spectra 1 to 17), the luminescence lifetime becomes longer. Single exponential functions were used to fit the data to obtain the luminescence lifetimes ( $\tau$ ), and the data are shown in Table 2.

## 4. DISCUSSION

**4.1. Hydration Number of Eu(III) Species.** It is known that the quenching of the luminescence of Eu(III) in aqueous solutions is due to the efficient energy transfer from the excited state ( ${}^5\text{D}_0$ ) of Eu(III) to the O–H vibration of the coordinated water molecules. Therefore, there is a correlation between the luminescence lifetime and the hydration number of Eu(III) in the

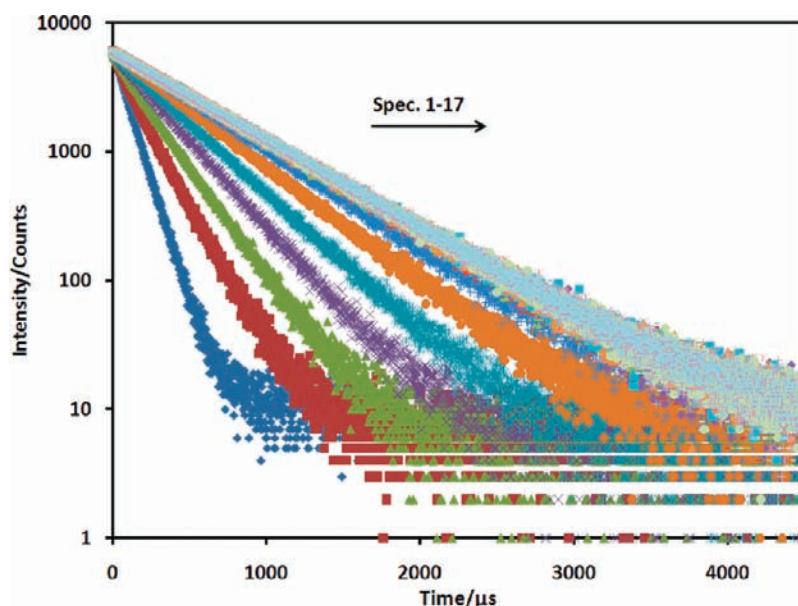


**Figure 6.** Luminescence decay of Eu(III)/DTPA solutions, same experimental conditions as for Figure 3. From Spectra 1 to 17, the ratio of  $C_{\text{DTPA}}/C_{\text{Eu}}$  increases from 0 to 3.

**Table 2.** Luminescence Lifetime and the Average Hydration Number of Eu(III) in Eu(III)/DTPA Solutions ( $C_{\text{Eu}} = 5\text{--}8 \text{ mmol} \cdot \text{dm}^{-3}$ ,  $I = 1.0 \text{ mol} \cdot \text{dm}^{-3} \text{ NaClO}_4$ ,  $\lambda_{\text{ex}} = 394 \text{ nm}$ ,  $\lambda_{\text{em}} = 615\text{--}620 \text{ nm}$ )

$C_{\text{L}}/C_{\text{Eu}}$	$\tau_{\text{exp}}, \mu\text{s}$	$n_{\text{H}_2\text{O,exp}} (\pm 0.5)$	% Eu species			$n_{\text{H}_2\text{O,cal}}$		
			$\text{Eu}^{3+}$	$\text{EuL}^{2-}$	$\text{Eu(HL)}^-$	assuming $\text{Eu(HL)} \cdot 3\text{H}_2\text{O}$	assuming $\text{Eu(HL)} \cdot 1.5\text{H}_2\text{O}$	assuming $\text{Eu(HL)} \cdot \text{H}_2\text{O}$
1.118	560.0	1.33	2.8	34.7	62.6	2.47	1.53	1.22
1.304	601.0	1.20	0.5	41.6	57.9	2.20	1.33	1.04
1.491	616.0	1.15	0.1	49.5	50.4	2.02	1.26	1.01
1.677	626.0	1.13	0	57.4	42.5	1.85	1.21	1.00
1.863	629.0	1.12	0	64.6	35.4	1.71	1.18	1.00
2.050	633.0	1.11	0	70.8	29.2	1.58	1.15	1.00
2.236	633.0	1.11	0	76.1	23.9	1.48	1.12	1.00
2.422	635.0	1.10	0	80.6	19.4	1.39	1.10	1.00
2.609	638.0	1.10	0	84.4	15.6	1.31	1.08	1.00
2.795	639.0	1.09	0	87.6	12.4	1.25	1.06	1.00
2.981	638.4	1.09	0	90.3	9.7	1.19	1.05	1.00

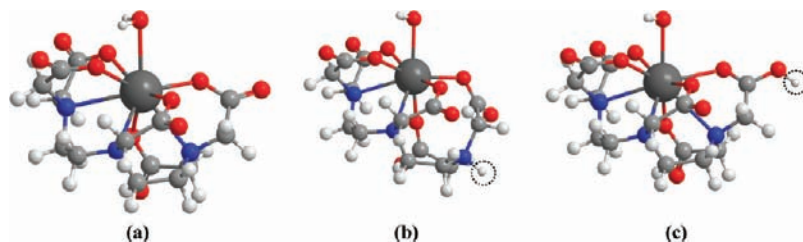


**Figure 7.** Optimized structures of the octa-dentate  $\text{Eu(DTPA)}^{2-}$  complex (a), the protonated  $\text{Eu(HDTPA)}^-$  complex where the protonation occurs on the amine nitrogen (b), and the protonated  $\text{Eu(HDTPA)}^-$  complex where the protonation occurs on the carboxylate oxygen (c). Black, Eu; red, oxygen; blue, nitrogen; gray, carbon; white, hydrogen. The position of protonation is indicated with a dashed circle. The energy of structure (b) is higher than that of the structure (c) by about 0.62 eV.

inner coordination sphere.<sup>28</sup> Using the lifetime data from this work (Table 2) and the previously established linear correlation between the luminescence lifetime and the hydration number of Eu(III) ( $n_{\text{H}_2\text{O}} = 1.05 \times \tau^{-1} - 0.7$ , where  $\tau$  is in milliseconds<sup>29</sup>),

the hydration number per Eu(III) in the solution,  $n_{\text{H}_2\text{O,exp}}$ , was determined (Table 2). The gradual decrease in the hydration number per Eu(III) with the increase in the concentration of DTPA, as shown in Table 2, indicates that the water molecules in

the inner coordination sphere of  $\text{Eu}^{3+}$  is gradually replaced by DTPA.

#### 4.2. Coordination Modes in the Eu(III)/DTPA Complexes.

The values of  $n_{\text{H}_2\text{O},\text{exp}}$  represent the average hydration number of all Eu(III) species in solution, including free  $\text{Eu}^{3+}$ ,  $\text{EuL}^{2-}$ , and  $\text{EuHL}^-$ . Of these species, the free  $\text{Eu}^{3+}$  is known to have 9 water molecules in the inner coordination sphere ( $n_{\text{H}_2\text{O}} = 9$ ).<sup>29,30</sup> The 1:1 Eu(III)/DTPA complex,  $\text{EuL}^{2-}$ , has been shown to be an octa-dentate chelate complex in which the DTPA coordinates to Eu(III) with five carboxylate oxygen atoms and three amine nitrogen atoms, leaving one position for a water molecule ( $n_{\text{H}_2\text{O}} = 1$ ).<sup>30–34</sup> In contrast, the hydration number in the protonated Eu(III)/DTPA complex,  $\text{EuHL}^-$ , remains uncertain. A hexa-dentate chelate complex for  $\text{LaHL}^-$  or  $\text{YbHL}^-$ , implying  $n_{\text{H}_2\text{O}} = 3$ , has previously been suggested but not substantiated with experimental evidence.<sup>35</sup> The luminescence lifetime data in conjunction with the DFT calculations in this work, as discussed below, could help to clarify the coordination mode and hydration number of the protonated Eu(III)/DTPA complex.

Geometry optimization of the structures of  $\text{EuL}^{2-}$  and  $\text{EuHL}^-$  complexes (where L stands for DTPA) were performed with DFT calculations. The optimized structures and the bond lengths are shown in Figure 7 and Table 3, respectively. The

**Table 3.** Calculated Eu–N and Eu–O Bond Lengths (Å) in the Eu(III)/DTPA Complexes

	$\text{EuDTPA}^{2-}$ (Figure 7a)	$\text{EuH(DTPA)}^-$ with H on N (Figure 7b)	$\text{EuH(DTPA)}^-$ with H on O (Figure 7c)
Eu–N1	2.893	4.129	3.042
Eu–N2	2.761	2.917	2.709
Eu–N3	2.873	2.747	2.734
Eu–O1	2.365	2.435	2.616
Eu–O2	2.435	2.357	2.382
Eu–O3	2.402	2.381	2.370
Eu–O4	2.505	2.401	2.402
Eu–O5	2.448	2.389	2.403
Eu–O6	2.673	2.530	2.550

structure of  $\text{EuL}^{2-}$  (Figure 7a) is optimized from the crystallographic data for this complex in the literature without the counterions.<sup>34</sup> Using the optimized structure of  $\text{EuL}^{2-}$  as a starting point, the structures of  $\text{EuHL}^-$  were further optimized by placing the proton on either the nitrogen of one amine group (Figure 7b) or the oxygen of one carboxylate group (Figure 7c).

In the structure of  $\text{EuL}^{2-}$ , the DTPA ligand is octa-dentate with five oxygen atoms from the carboxylate groups and three nitrogen atoms from the amine groups coordinating to Eu(III). One water molecule is in the inner coordination sphere of Eu(III), satisfying the total coordination number of 9 (Figure 7a). The oxygen atoms from the carboxylate groups and water are considerably closer to the central Eu atom ( $R_{\text{Eu–O}} = 2.365$  to  $2.673$  Å) than the nitrogen atoms from the amine groups ( $R_{\text{Eu–N}} = 2.761$  to  $2.893$  Å).

In the optimized structure of  $\text{EuHL}^-$  with the proton on the nitrogen of one amine group (Figure 7b), the nitrogen atom moves away from the Eu atom with  $R_{\text{Eu–N1}} = 4.129$  Å. This is understandable because the basicity of this amine group would be greatly reduced upon protonation and amine coordination to Eu(III) becomes impossible. Therefore, the  $\text{EuHL}^-$  complex can be described essentially as being hepta-dentate with DTPA. The hydration number of the hepta-dentate  $\text{EuHL}^-$  complex could remain to be  $n_{\text{H}_2\text{O}} = 1$ , because the Eu(III) is well-“enveloped” by the DTPA ligand and is not readily accessed by additional water molecules.

If the protonation occurs on the oxygen of one carboxylate group (Figure 7c), considerable changes in some of the Eu–O and Eu–N distances are observed in the optimized structure of  $\text{EuHL}^-$ . Most notably, the Eu–O1 and Eu–N1 distances become longer ( $R_{\text{Eu–O1}}$  from  $2.365$  to  $2.616$  Å,  $R_{\text{Eu–N1}}$  from  $2.893$  to  $3.042$ ), indicating significant weakening of these two coordination bonds. However, all three nitrogen atoms and five oxygen atoms remain coordinated with Eu, and the DTPA ligand is still octa-dentate in the  $\text{EuHL}^-$  complex, with the hydration number  $n_{\text{H}_2\text{O}} = 1$ .

Besides optimizing the structures of the  $\text{EuHL}^-$  complex, DFT calculations in this work also show that the energy of the  $\text{EuHL}^-$  complex with the proton on the amine nitrogen (Figure 7b) is higher than that of the  $\text{EuHL}^-$  complex with

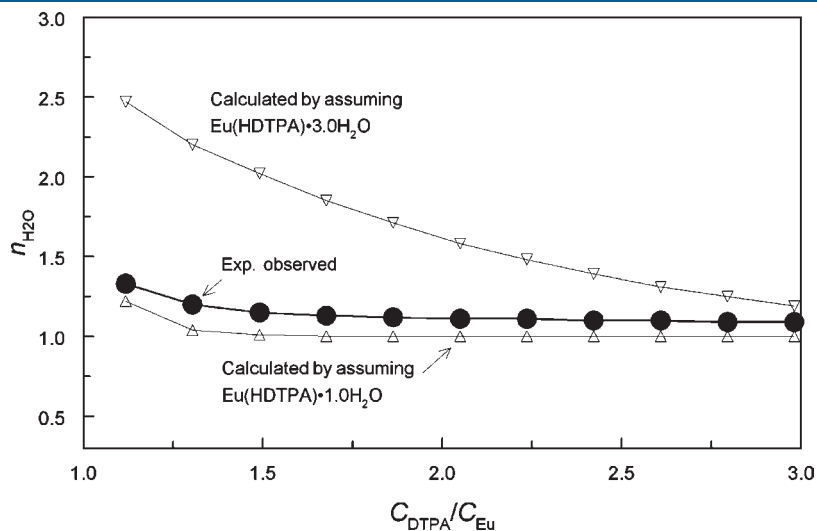


**Figure 8.** Comparison between the average hydration number determined by luminescence decay,  $n_{\text{H}_2\text{O},\text{exp}}$ , and the average hydration number calculated from speciation,  $n_{\text{H}_2\text{O},\text{cal}}$ .



the proton on the carboxylate oxygen (Figure 7c) by about 0.62 eV. Thus the latter, in which an octa-dentate ligand (DTPA) and a water molecule coordinating with Eu(III), is the more probable structure of the  $\text{EuHL}^-$  complex.

When it was assumed that the  $\text{EuHL}^-$  complex has a hydration number of 1.0 as the DFT calculation shows or 3.0 as a previous study<sup>35</sup> suggests, the average hydration number of Eu(III) in the Eu(III)/DTPA solutions could be obtained by a speciation calculation using the stability constants from this work. The speciation of Eu(III) and the calculated  $n_{\text{H}_2\text{O,cal}}$  are shown in Table 2. The values of  $n_{\text{H}_2\text{O,cal}}$  are compared with those of  $n_{\text{H}_2\text{O,exp}}$  determined by luminescence decay in Figure 8. It is evident that the experimental data do not support the formation of a hexa-dentate  $\text{EuHL}^-$  complex with  $n_{\text{H}_2\text{O}} = 3$  suggested in the literature.<sup>35</sup> The assumption of a  $\text{EuHL}^-$  complex with  $n_{\text{H}_2\text{O}} = 1$ , based on the results of DFT calculations, provides reasonably good agreement with the experimental data.

An anonymous reviewer made an interesting point by assuming that the protonation of the carboxylate group in the  $\text{EuHL}^-$  complex may lead to the dissociation of the Eu–O1 bond and the steric hindrance in the bulky complex system may prevent a facile rehydration of Eu, leaving the hydration number of Eu in the complex unchanged ( $n_{\text{H}_2\text{O}} = 1$ ). This assumption also seems to agree with the luminescence lifetime data. However, the experimentally observed structure of  $\text{Eu}(\text{DTPA})^{2-}$  (Figure 7a) and the DFT optimized structure of  $\text{EuH}(\text{DTPA})^-$  (Figures 7c) indicate that the steric hindrance around the dissociated Eu would be low and the hydration number of the Eu in such a “dissociated-protonated”  $\text{EuHL}^-$  complex would be most likely to become 2, inconsistent with the luminescence lifetime data. Therefore, we still think that the structure shown in Figure 7c reasonably depicts the  $\text{EuHL}^-$  complex.

## 5. SUMMARY

Thermodynamic data show that, in the temperature range from 10 to 70 °C, the trivalent lanthanides ( $\text{Nd}^{3+}$  and  $\text{Eu}^{3+}$ ) form two complexes with DTPA,  $\text{ML}^{2-}$ , and  $\text{MHL}^-$  where L denotes the fully deprotonated DTPA. The complexation is exothermic and becomes weaker as the temperature is increased. For the first time, integration of the experimental data from luminescence spectroscopy and the results of DFT calculations has led to the conclusion that the DTPA ligand in the  $\text{MHL}^-$  complex is probably octa-dentate with one protonated carboxylate group and one water molecule in the inner coordination sphere.

## ■ ASSOCIATED CONTENT

Supporting Information. A diagram of speciation of Eu(III) in the DTPA solution as a function of acidity. This material is available free of charge via the Internet at <http://pubs.acs.org>.

## ■ AUTHOR INFORMATION

### Corresponding Author

\*E-mail: LRao@lbl.gov.

## ■ ACKNOWLEDGMENT

The experimental work and the DFT calculations were supported, respectively, by the Fuel Cycle Research and Development Program

of Office of Nuclear Energy (NE FCR&D) and the Single Investigator and Small Group (SISGR) Program of the Office of Science, Office of Basic Energy Sciences, the U.S. Department of Energy (DOE), under Contract No. DE-AC02-05CH11231 at Lawrence Berkeley National Laboratory. Z.Z. of Stanford University thanks the National Nanotechnology Infrastructure Network (NNIN) for providing computational time for this work. L.R.M. acknowledges the support from DOE NE FCR&D Thermodynamics and Kinetics program, under DOE Idaho Operations Office Contract DE-AC07-05ID14517 while preparing this manuscript. The authors thank the anonymous reviewers whose comments have helped to improve this manuscript.

## ■ REFERENCES

- (1) Weaver, B.; Kappelman, F. A. . ORNL-3559, August, 1964.
- (2) Weaver, B.; Kappelman, F. A. *J. Inorg. Nucl. Chem.* **1968**, *30*, 263.
- (3) Nilsson, M.; Nash, K. L. *Solvent Extr. Ion Exch.* **2009**, *27*, 354.
- (4) Nilsson, M.; Nash, K. L. *Solvent Extr. Ion Exch.* **2007**, *25* (6), 665.
- (5) NIST Standard Reference Database 46: *NIST Critically Selected Stability Constants of Metal Complexes Database*, Version 8.0; U.S. Department of Commerce, 2004.
- (6) Harder, R.; Chaberek, S. J. *Inorg. Nucl. Chem.* **1959**, *11*, 197–209.
- (7) Choppin, G. R.; Thakur, P.; Mathur, J. N. C. *R. Chim.* **2007**, *10*, 910–928.
- (8) Baybarz, R. D. *J. Inorg. Nucl. Chem.* **1965**, *27*, 1831.
- (9) Gritmon, T. F.; Goedken, M. P.; Choppin, G. R. *J. Inorg. Nucl. Chem.* **1977**, *39*, 2021.
- (10) Tian, G.; Rao, L. *Sep. Sci. Technol.* **2010**, *45*, 1718.
- (11) Tian, G.; Martin, L. R.; Rao, L. *Inorg. Chem.* **2010**, *49*, 10598–10605.
- (12) Dean, J. A. *Analytical Chemistry Handbook*; McGraw-Hill, Inc.: New York, 1995, p 3–108.
- (13) Gran, G. *Analyst* **1952**, *77*, 661.
- (14) Zanonato, P.; Di Bernardo, P.; Bismondo, A.; Liu, G.; Chen, X.; Rao, L. *J. Am. Chem. Soc.* **2004**, *126*, 5515.
- (15) Di Bernardo, P.; Zanonato, P.; Tian, G.; Tolazzi, M.; Rao, L. *J. Chem. Soc., Dalton Trans.* **2009**, *23*, 4450.
- (16) Gao, P.; Sabatini, A.; Vacca, A. *Talanta* **1996**, *43*, 1739.
- (17) Hummel, W.; Anderegg, G.; Puigdomènech, I.; Rao, L.; Tochiyama, O. *Chemical Thermodynamics of Compounds and Complexes of: U, Np, Pu, Am, Tc, Zr, Ni and Se with Selected Organic Ligands*; Mompean, F. J., Illemassene, M., Perrone, J., Eds.; Elsevier B.V.: Amsterdam, 2005.
- (18) Rao, L.; Srinivasan, T. G.; Garnov, A. Yu.; Zanonato, P.; Di Bernardo, P.; Bismondo, A. *Geochim. Cosmochim. Acta* **2004**, *68*, 4821.
- (19) Arnek, R. *Ark. Kemi* **1970**, *32*, 81.
- (20) Perdew, J. P.; Burke, K.; Ernzerhof, M. *Phys. Rev. Lett.* **1996**, *77*, 3865.
- (21) Valiev, M.; Bylaska, E. J.; Govind, N.; Kowalski, K.; Straatsma, T. P.; van Dam, H. J. J.; Wang, D.; Nieplocha, J.; Apra, E.; Windus, T. L.; de Jong, W. A. *Comput. Phys. Commun.* **2010**, *181*, 1477.
- (22) Kühle, W.; Dolg, M.; Stoll, H.; Preuss, H. *J. Chem. Phys.* **1994**, *100*, 7535–7542.
- (23) EMSL Basis Set Library (<http://www.emsl.pnl.gov/forms/basisform.html>).
- (24) Jørgensen, C. K. *Absorption Spectra and Chemical Bonding in Complexes*, Pergamon Press, London, 1962.
- (25) Jørgensen, C. K.; Judd, B. R. *Mol. Phys.* **1964**, *8*, 281.
- (26) Judd, B. R. . In *Handbook on the Physics and Chemistry of Rare Earths*; Gschneidner, K. A., Jr., Eyring, L., Eds.; North-Holland: Amsterdam, 1988; Vol. 11, Ch. 74.
- (27) Mason, S. F.; Peacock, R. D.; Stewart, B. *Chem. Phys. Lett.* **1974**, *29*, 149.
- (28) Horrocks, W. DeW., Jr.; Sudnick, D. R. *J. Am. Chem. Soc.* **1979**, *101*, 334.
- (29) Barthelemy, P. P.; Choppin, G. R. *Inorg. Chem.* **1989**, *28*, 3354.

- (30) Kimura, T.; Choppin, G. R. *J. Alloys Compd.* **1994**, *213*, 313.
- (31) Mondry, A.; Starynowicz, P. *Polyhedron* **2000**, *19*, 771.
- (32) Inomata, Y.; Sunakawa, T.; Howell, F. S. *J. Mol. Struct.* **2003**, *648*, 81.
- (33) Bryden, C. C.; Reilley, C. N. *Anal. Chem.* **1982**, *54*, 610.
- (34) Liu, B.; Wang, Y. F.; Wang, J.; Gao, J.; Xu, R.; Kong, Y. M.; Zhang, L. Q.; Zhang, X. D. *J. Struct. Chem.* **2009**, *50*, 880–886.
- (35) Harder, R.; Chaberek, S. *J. Inorg. Nucl. Chem.* **1959**, *11*, 197–209.

#### ■ NOTE ADDED AFTER ASAP PUBLICATION

This paper was published on the Web on March 4, 2011, with the incorrect artwork for the abstract graphic. The corrected version was reposted on March 9, 2011.